REPORT DOCUMENTATION PAGE

Form Approved OMB NO. 0704-0188

The public reporting burden for this collection of information is estimated to average 1 hour per response, including the time for reviewing instructions, searching existing data sources, gathering and maintaining the data needed, and completing and reviewing the collection of information. Send comments regarding this burden estimate or any other aspect of this collection of information, including suggesstions for reducing this burden, to Washington Headquarters Services, Directorate for Information Operations and Reports, 1215 Jefferson Davis Highway, Suite 1204, Arlington VA, 22202-4302. Respondents should be aware that notwithstanding any other provision of law, no person shall be subject to any oenalty for failing to comply with a collection of information if it does not display a currently valid OMB control number.
PLEASE DO NOT RETURN YOUR FORM TO THE ABOVE ADDRESS.

1. REPORT DATE (DD-MM-YYYY)	2. REPORT TYPE	3. DATES COVERED (From - To)
	New Reprint	-

4. TITLE AND SUBTITLE	5a. CONTRACT NUMBER
Digitally Driven Antenna for HF Transmission	
	5b. GRANT NUMBER
	W911NF-04-D-0001
	5c. PROGRAM ELEMENT NUMBER
	611102

6. AUTHORS	5d. PROJECT NUMBER
Steven D. Keller, W. Devereux Palmer, William T. Joines	
	5e. TASK NUMBER
	5f. WORK UNIT NUMBER

7. PERFORMING ORGANIZATION NAMES AND ADDRESSES	8. PERFORMING ORGANIZATION REPORT NUMBER
Duke University 130 Hudson Hall, Box 90271 Duke University Durham, NC 27705 -	

9. SPONSORING/MONITORING AGENCY NAME(S) AND ADDRESS(ES)	10. SPONSOR/MONITOR'S ACRONYM(S)
U.S. Army Research Office P.O. Box 12211 Research Triangle Park, NC 27709-2211	ARO
	11. SPONSOR/MONITOR'S REPORT NUMBER(S)
	49428-EL-SR.11

12. DISTRIBUTION AVAILIBILITY STATEMENT

Approved for public release; distribution is unlimited.

13. SUPPLEMENTARY NOTES

The views, opinions and/or findings contained in this report are those of the author(s) and should not contrued as an official Department of the Army position, policy or decision, unless so designated by other documentation.

14. ABSTRACT

An electrically small antenna connected directly to a complementary pair of switching transistors is driven with a pulsewidth modulated HF signal, eliminating the requirement for a frequency-dependent impedance-matching network. The intrinsic reactance of the transmit and receive antennas acts as a filter to recover the HF signal from the digital pulse train. This is defined here as the digitally driven antenna architecture. A circuit simulator with broadband equivalent-circuit models for the transmit and receive antennas is used to predict the received signal in

15. SUBJECT TERMS

Antenna, communication system, electricallysmall, HF, pulsewidth modulation, switching amplifier, VHF

16. SECURITY CLASSIFICATION OF:			17. LIMITATION OF ABSTRACT	15. NUMBER OF PAGES	19a. NAME OF RESPONSIBLE PERSON
a. REPORT	b. ABSTRACT	c. THIS PAGE			Dev Palmer
UU	UU	UU	UU		19b. TELEPHONE NUMBER
					919-549-4246

Standard Form 298 (Rev 8/98)
Prescribed by ANSI Std. Z39.18

Report Title

Digitally Driven Antenna for HF Transmission

ABSTRACT

An electrically small antenna connected directly to a complementary pair of switching transistors is driven with a pulsewidth modulated HF signal, eliminating the requirement for a frequency-dependent impedance-matching network. The intrinsic reactance of the transmit and receive antennas acts as a filter to recover the HF signal from the digital pulse train. This is defined here as the digitally driven antenna architecture. A circuit simulator with broadband equivalent-circuit models for the transmit and receive antennas is used to predict the received signal in the time domain, and the expected received spectrum is calculated using Maxwell's equations and the fast Fourier transform. The simulated circuit is realized using a highly capacitive electrically small dipole antenna driven at 1 MHz with a 10-MHz reference signal on the pulsewidth modulator as the transmitter and a highly inductive 470- H ferrite-loaded loop as the receive antenna. The 1-MHz signal is clearly evident in the time-domain received signal on an oscilloscope, and also in the received spectrum, as observed on a spectrum analyzer. This demonstrates that indeed it may be possible to produce efficient radiation across a wide bandwidth from an electrically small antenna by driving the antenna directly with a digital pulse train.

REPORT DOCUMENTATION PAGE (SF298)
(Continuation Sheet)

Continuation for Block 13

ARO Report Number   49428.11-EL-SR
Digitally Driven Antenna for HF Transmission   ...

Digitally Driven Antenna for HF Transmission

Steven D. Keller, *Member, IEEE*, W. Devereux Palmer, *Senior Member, IEEE*, and
William T. Joines, *Life Fellow, IEEE*

Abstract—An electrically small antenna connected directly to a complementary pair of switching transistors is driven with a pulsewidth modulated HF signal, eliminating the requirement for a frequency-dependent impedance-matching network. The intrinsic reactance of the transmit and receive antennas acts as a filter to recover the HF signal from the digital pulse train. This is defined here as the digitally driven antenna architecture. A circuit simulator with broadband equivalent-circuit models for the transmit and receive antennas is used to predict the received signal in the time domain, and the expected received spectrum is calculated using Maxwell's equations and the fast Fourier transform. The simulated circuit is realized using a highly capacitive electrically small dipole antenna driven at 1 MHz with a 10-MHz reference signal on the pulsewidth modulator as the transmitter and a highly inductive 470-μH ferrite-loaded loop as the receive antenna. The 1-MHz signal is clearly evident in the time-domain received signal on an oscilloscope, and also in the received spectrum, as observed on a spectrum analyzer. This demonstrates that indeed it may be possible to produce efficient radiation across a wide bandwidth from an electrically small antenna by driving the antenna directly with a digital pulse train.

Index Terms—Antenna, communication system, electrically small, HF, pulsewidth modulation, switching amplifier, VHF.

I. INTRODUCTION

AS semiconductor technology has matured over the years, the incorporation of active devices such as transistor amplifiers with passive antenna elements has become an increasingly fertile topic of interest, enabling increased system bandwidth and reduced system size [1]. Extensive research has been conducted on the integration of antenna structures with linear push–pull power amplifiers [2], such as Class AB [3] and Class B [4] amplifiers, to yield fully integrated active antennas that offer efficiencies of between 55%–65%. While this research has yielded some significant advances in the area of active antennas, the limitation of its scope to linear amplifier classes has, in turn, limited the maximum achievable power efficiencies of the resulting active antenna systems.

A chief concern of merging an antenna structure with a higher efficiency amplifier, such as a switching Class D amplifier driven by an RF carrier modulated with a desired information signal and then encoded into a digital pulse train, is that a narrowband filtering mechanism still is needed between the amplifier output and the load in order to suppress the switching signal and harmonics and recover the modulated carrier. Additionally, if the antenna is electrically small compared to the wavelength of the radiated signal [5], it has been shown that under traditional linear operation, such an antenna can only operate over a moderate bandwidth with very low efficiency [6], [7]. However, the capacitive reactance of the electrically small antenna serves as an effective output filter that aides in recovery of the original baseband signal at the output of the switching amplifier without using a narrowband filtering circuit, and consequently provides high-efficiency power transfer to the antenna without reducing its operational bandwidth or radiation efficiency. This technique was first proposed by Merenda [8], [9], who developed the theory and initially demonstrated the concept at audio frequencies. Its application at RF frequencies, where it will have the most impact on the size and performance of a communication system, is the focus of this paper. A proof-of-concept that the digitally driven antenna (DDA) architecture can be used with an electrically small antenna to transmit an HF signal without the need for conjugate impedance matching will be presented. A quantitative evaluation of the DDA architecture efficiency is under investigation and will be reported in a future paper.

The circuit in Fig. 1 defines the difference between the standard heterodyne radio architecture and the new architecture, which is formally established in this work as the DDA architecture. The generation of the modulated carrier is the same in both architectures, as is the antenna. The distinguishing difference is that while in the heterodyne architecture the signal remains analog and is amplified using a linear amplifier with an impedance matching network, in the DDA architecture the antenna is driven by an encoded digital pulse train whose power is amplified by a complementary pair of switching transistors.

This circuit draws from techniques developed for modern Class D power amplifiers in order to drive an antenna with a pulsewidth modulated HF signal at maximized power efficiency. The proposed communication system will begin with an HF band RF signal, amplitude modulated with a desired information signal. This RF signal is then pulsewidth modulated and sent to the base terminals of two semiconductor switching devices, such as bipolar junction transistors (BJTs) or MOSFETs. Since the transistor switches operate in either cutoff or saturation due to the digital pulsewidth modulation bias signal, there is no quiescent transistor bias current and the power efficiency for the system is increased.
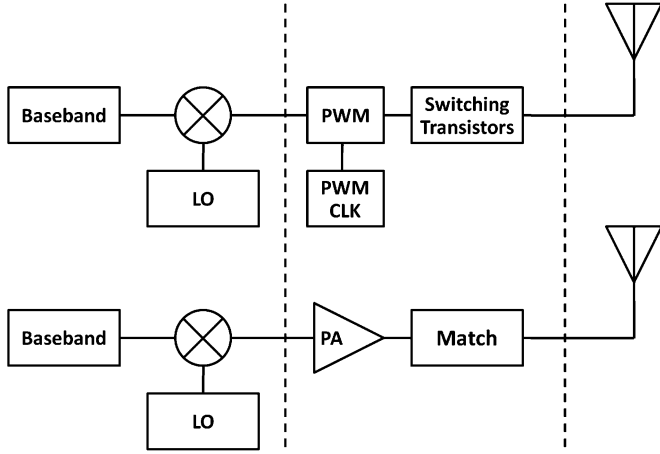
Fig. 1. (*top*) DDA architecture versus (*bottom*) standard heterodyne radio transmitter architecture. Note that the power amplifier and matching network in the standard circuit are replaced by a pulsewidth modulator (PWM) and switching transistors in the DDA system.

The spectrum of this output digital signal is composed of the original modulated carrier signal, the sampling clock signal for the pulsewidth modulator (typically a sawtooth or triangle wave), and various harmonics and intermodulation products. A filtering mechanism at the amplifier output prior to the load, typically in the form of an *L–C* low-pass filter, is traditionally employed to suppress the switching signal and its harmonics within the amplified output signal and to pass only an amplified form of the modulated carrier signal to the load. In this experiment, however, no discrete filtering mechanism will be included. Instead, the implicit reactance of the antenna system will be used as the filtering mechanism through which the modulated carrier signal is recovered.

II. SYSTEM DESIGN AND MODELING

A. System Design

A DDA system was designed to transmit an unmodulated 1-MHz carrier and system performance was modeled using a circuit simulator. The crux of the DDA system is the pulsewidth modulator and the complementary pair of switching transistors. The fidelity of the recovered signal on the receiver end relies strongly on the accuracy of the pulsewidth modulator output and the switching capabilities of the transistors. Thus, great care must be taken in the design of this circuit to ensure the proper functionality of the complete DDA system.

The discrete passive and active components for this design are shown in Table I. The Maxim MAX999 comparator was chosen for its high-speed operation with 2.3-ns rise and fall times and a maximum propagation delay of 8.5 ns. The decoupling capacitor values, 0.1 and 1 μF, were selected based on the recommendations found in [10] in order to stabilize the power supply voltage at the comparator chip. The Fairchild MMBT5770 NPN BJT and the Fairchild MMBTH81 PNP BJT were selected based on their switching capabilities, each with an f_T of 600 MHz, fast enough for operation in the HF/VHF frequency range. SPICE

TABLE I
DDA SYSTEM CLASS-D AMPLIFIER COMPONENT LIST

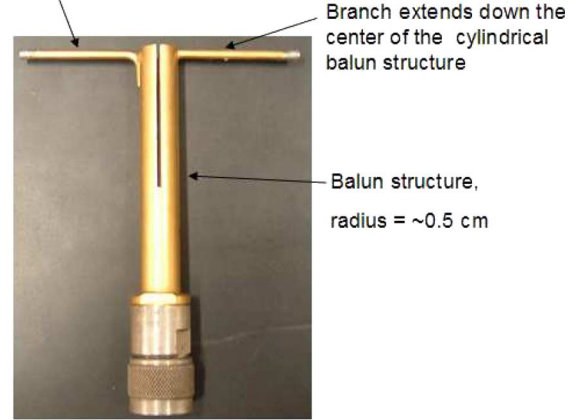| Component	Company / Model #
High-Speed Comparator	*Maxim* MAX999
NPN RF Transistor	*Fairchild Semiconductor* MMBT5770
PNP RF Transistor	*Fairchild Semiconductor* MMBTH81
0.1 μF Capacitor	*Nichicon* F921V104MAA
1 μF Capacitor	*Nichicon* F931A106MAA
50 Ω Resistor	*Vishay Dale* CRCW251249R9FKEG

Fig. 2. Electrically small dipole antenna with a cylindrical balun.
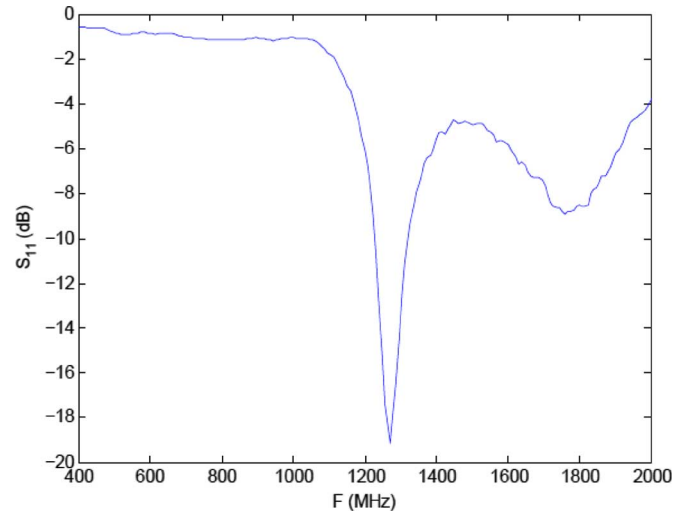

Fig. 3. S_{11} plot for DDA system transmit dipole antenna.

models that accurately predict device performance are readily available for these parts.

A dipole antenna with a cylindrical balun was selected as the transmit antenna, as shown in Fig. 2. The dipole arms have a radius of 0.15 cm and a total length of approximately 9.1 cm. The reflection coefficient plot for this antenna, shown in Fig. 3, indicates that under traditional operation, the antenna has a resonant frequency of about 1.26 GHz. However, at the DDA carrier frequency of 1 MHz, this antenna is approximately $\lambda/3300$ in length, which certainly qualifies it as electrically small.

A ferrite rod loop antenna, typically used for reception of low-frequency AM radio signals between 520–1610 kHz, was
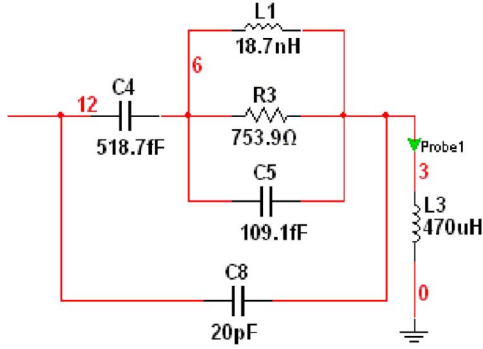
Fig. 4. Discrete component model of electrically small dipole transmit antenna, including the balun capacitance, and the inductance of the loop stick receive antenna.
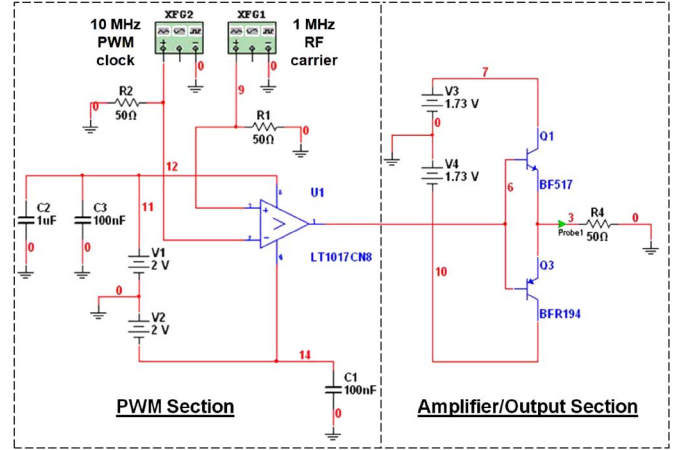

Fig. 5. Schematic of complete DDA system as represented in National Instruments' Multisim Circuit Design program. Transmit and receive antenna models from Fig. 4 are substituted for the 50-Ω resistor $R4$ in the simulation of the full DDA system.

selected as the receive antenna. This type of antenna is highly inductive; the antenna used in this experiment can be modeled as a 470-μH inductor.

B. System Circuit Model

A variety of models have been developed for electrically small antennas such as one based on spherical waves [11] and another utilizing broadband lumped elements [12]. However, according to [13], these models have greater than 30% error for antennas with a dipole length less than $\lambda/5$ when compared with analytical solutions from [14] and [15]. The empirical formulas determined in [13] and [16] may be used to establish a four-element model of an electrically small dipole antenna that is highly accurate for an antenna with length less than 0.2λ. Based on the existing literature, the optimal model available for simulation of the $\lambda/3300$ dipole antenna used in the DDA system experiment is shown in [13, Fig. 3]. Using a dipole arm length $h = 4.055$ cm and radius $a = 0.15$ cm, the final lumped-element model has the corresponding values $C_4 = 519$ fF, $L_1 = 18.7$ nH, $R_3 = 753.9$ Ω, and $C_5 = 109$ fF.

Additional capacitance must be added to this model to account for the capacitance of the cylindrical balun structure. Using the balun radius of 0.5 cm and length of 8 cm, the added capacitance can be approximated by using the formula for the capacitance between two concentric cylinders

$$C_{\text{cylinder}} = \frac{2\pi\varepsilon_0}{\ln\left(\frac{b}{a}\right)} \cdot L = 8.5 \text{ pF}. \tag{1}$$

Thus, at least 8.5 pF of extra capacitance needs to be added to the existing circuit model of the dipole antenna in order to produce an accurate simulation of the DDA system. By examining the spectral simulation results for added capacitance ranging from 8.5 to 40 pF, it was found that 20 pF produced the closest match to the experimental results. The additional 11.5 pF likely is due to the fringing fields between the tuning slots along two sides of the balun and from the balun edge at the dipole antenna junction. The complete circuit model of the transmit dipole antenna with added balun capacitance and the output inductive loop antenna is shown in Fig. 4.

Performance of the complete circuit including the transmit and receive antennas was modeled using National Instruments'

Multisim Circuit Design program. The schematic is shown in Fig. 5. The XFG1 device generates a 1-MHz sine wave that is sent to the noninverting input of the MAX999 comparator, while the XFG2 device generates a 10-MHz triangle wave that is sent to the inverting input. Both input signals were set to 1 V_{pp}, consistent with the operating parameters of the comparator. The comparator output is a digital pulsewidth modulated signal with a duty cycle that varies according to the amplitude of the 1-MHz carrier signal. This signal is then fed into the base terminals of an NPN/PNP transistor pair arranged in a push–pull configuration. A dual voltage power supply, $V_0 = +/-1.73$ V, is connected to the system with the positive voltage connected to the collector terminal of the NPN transistor and the negative voltage connected to the collector terminal of the PNP transistor.

Since it was not possible to explicitly simulate the radiation of the time-domain input signal from the electrically small dipole to the ferrite rod loop antenna, the approximate simulated spectrum of the received signal was calculated from the current passing through the antenna system output i_{probe1}. First, this current was recorded for 100 cycles of the 1-MHz input signal. Next, this data was used to yield an approximation of the spectrum of the received signal by applying Maxwell's equations governing antenna radiation and reception and the fast Fourier transform (FFT). From Ampere's Law,

$$\nabla \times H = \varepsilon \frac{\partial E}{\partial t} + J \tag{2}$$

it is seen that the magnetic field H is proportional to the current density J, which can be associated with i_{probe1} in the Multisim simulation such that

$$H \propto i_{\text{probe1}}. \tag{3}$$

From Faraday's Law, the voltage at the terminals of the receive antenna is

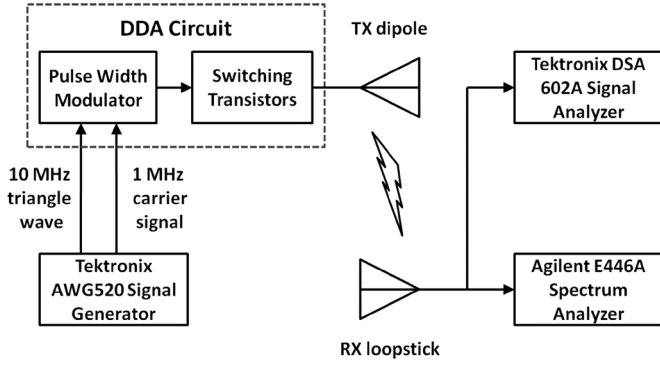$$\nabla \times E = -\mu \frac{\partial H}{\partial t} \tag{4}$$

Fig. 6. Diagram of the experimental setup used to evaluate the performance of the complete DDA system.
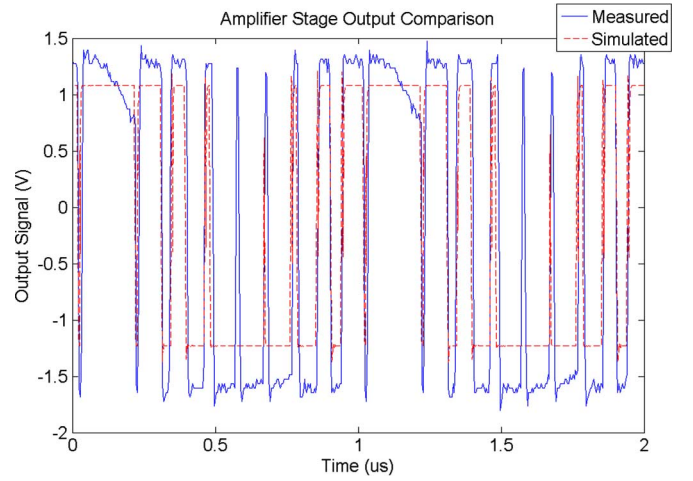

Fig. 7. Comparison of measured and simulated output with the dipole antenna disconnected and the switching transistors terminated with a 50-Ω resistor. Pulsewidth modulation by the 1-MHz carrier signal is clearly visible.
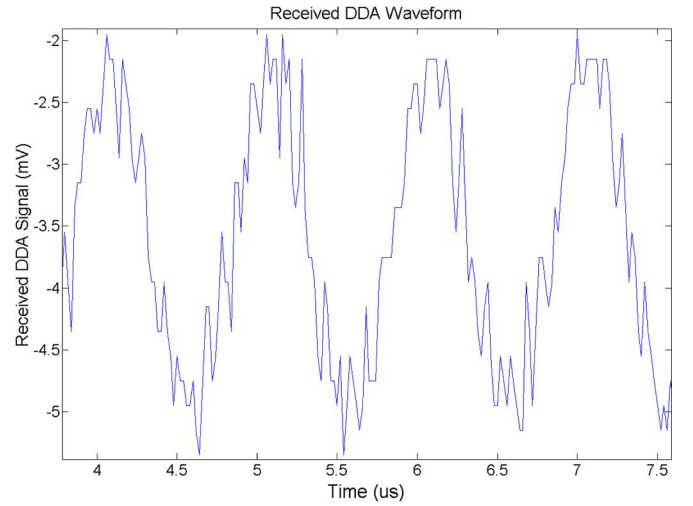

Fig. 8. Measured time-domain output of full DDA system.

and so the following approximation is obtained by substituting i_{probe1} for H in (4):

$$\text{Received signal} = \nabla \times E \propto -\mu \frac{\partial i_{\mathrm{probe1}}}{\partial t}. \tag{5}$$

Thus, by taking the time derivative of the simulated current through the antenna model, multiplying by μ_0 to properly scale the value for free-space radiation, and performing an FFT on the resulting signal, an approximate frequency-domain representation of the received signal was obtained for the simulated DDA system. Simulation results will be shown and compared to experimental measurements in Section III.

III. EXPERIMENTAL SETUP AND RESULTS

Fig. 6 shows a diagram of the experimental setup used to evaluate the performance of the DDA system. The Tektronix AWG520 arbitrary waveform generator simultaneously provides a 1-MHz carrier signal and a 10-MHz triangle wave PWM reference signal, both with a peak-to-peak voltage of 1 V, to the comparator listed in Section II in order to achieve pulse modulation. The pulsewidth modulated signal is amplified by the switching transistors and used to drive the electrically small dipole antenna. The signal transmitted by the dipole is received by the ferrite rod loop antenna a short distance away. For an electrically small transmitting antenna, far-field measurement of a 1-MHz carrier would require the transmit and receive antennas to be

$$r_{\mathrm{far}} > \frac{\lambda}{2\pi} \approx 48 \text{ m}. \tag{6}$$

With the existing laboratory space, the experimental measurements were limited to the reactive near field and were made with the dipole antenna approximately 15–20 cm away from the ferrite rod loop antenna in order to minimize additional amplification components on the receive end of the system. The received signal is displayed on Agilent's E4446A spectrum analyzer and Tektronix's DSA 602A digitizing signal analyzer in order to simultaneously observe the spectrum and time-domain waveform of the received signal.

To evaluate the performance of the pulsewidth modulator and the switching transistors separately, the antenna models in the simulation both were replaced with a single 50-Ω resistor and

the model output was recorded for 10 μs. The dipole antenna was disconnected and the experimental output of the switching transistors also was recorded on the DSA 602A. A comparison of the simulated and measured results is shown in Fig. 7. The pulsewidth modulation corresponding to the 1-MHz carrier signal is clearly visible. Due to variability in the experimental load impedance, the amplitude of the measured signal is slightly higher than the Multisim simulation results. Some slight ringing is observed at the pulse transition points from low to high and high to low, but the amplified pulses are generally stable and compare favorably with the simulated results.

With the key component performance validated through modeling and experiment, the dipole was reconnected and the complete DDA system was tested by measuring the signal received by the ferrite rod loop antenna. The time-domain received signal is shown in Fig. 8.

The received nonamplified signal is relatively small at approximately 3-mV peak-to-peak. This is most likely due to the large impedance mismatch between the receive antenna, approximately $j2950$ Ω at 1 MHz, and the 50-Ω instrumentation
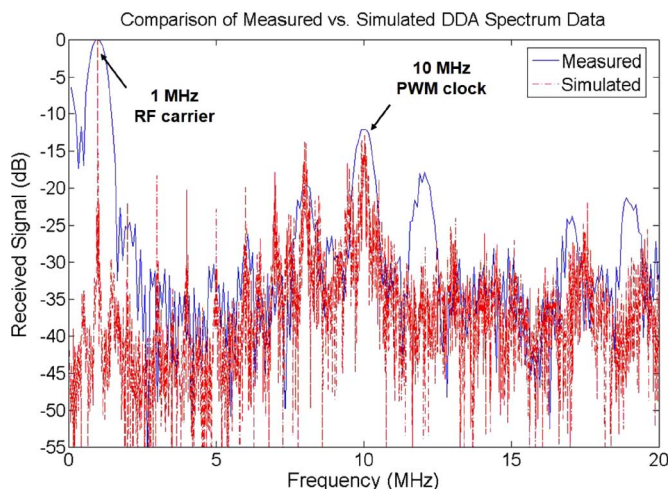
Fig. 9. Comparison of measured and normalized simulation spectrum data from the complete DDA system.

inputs. Despite the small amplitude of the received signal, the original 1-MHz baseband signal is distinctly visible within this measured data.

A comparison of the normalized measured spectrum with the expected received spectrum as calculated from the circuit simulator output described in Section II is shown in Fig. 9. The simulation results validate the amplitude and frequency of the 1-MHz carrier wave, harmonics, and intermodulation products. As expected from the time-domain measurements, the 1-MHz carrier signal again is dominant. The harmonics and intermodulation products associated with the pulsewidth modulation of the carrier signal still are evident in the final received signal spectrum, although they are considerably reduced in amplitude. The strongest of these higher frequency signals is the 10-MHz pulsewidth modulator reference signal at about 12 dB down from the 1-MHz carrier.

IV. CONCLUSION

This paper has defined the DDA architecture as first proposed by Merenda and demonstrates the viability of the technique at HF frequencies through simulation and measurement of a DDA system designed to transmit a 1-MHz signal through an electrically small (approximately $\lambda/3300$) antenna. In this experiment, the power amplifier and matching network used in the typical heterodyne radio architecture were replaced by a pulsewidth modulator and a pair of switching transistors. Transmission of the 1-MHz carrier was clearly evident in both the simulated and measured data. Additionally, a circuit model for a DDA system has been developed and time-domain simulation results of this model validate the experimental data. Since the measured amplitudes of the harmonics and intermodulation products associated with the pulsewidth modulation of the carrier signal in this first design are much higher than those necessary to meet standard Federal Communications Commission (FCC) transmission requirements, future research of this technique and refinement of this circuit design should focus on techniques to reduce these

signal amplitudes down to acceptable levels. While many unanswered questions about this technique remain, this proof of concept experiment demonstrates the possibility of achieving a dramatic reduction in the size and signature of antennas for mobile wireless communications systems. Further exploration of this technique through refinement of the proposed model and experimentation may lead to a revolutionary transceiver system capable of efficient radiation across a wide bandwidth from an electrically small antenna.

REFERENCES

[1] J. Lin and T. Itoh, "Active integrated antennas," *IEEE Trans. Microw. Theory Tech.*, vol. 42, no. 12, pp. 2186–2194, Dec. 1994.
[2] V. Radisic, Y. Qian, and T. Itoh, "Novel architectures for high efficiency amplifiers for wireless applications," *IEEE Trans. Microw. Theory Tech.*, vol. 46, no. 11, pp. 1901–1909, Nov. 1998.
[3] W. R. Deal, V. Radisic, Y. Qian, and T. Itoh, "Integrated-antenna push–pull power amplifiers," *IEEE Trans. Microw. Theory Tech.*, vol. 47, no. 8, pp. 1418–1424, Aug. 1999.
[4] V. Radisic, S. T. Chew, Y. Qian, and T. Itoh, "High-efficiency power amplifier integrated with antenna," *IEEE Microw. Guided Wave Lett.*, vol. 7, no. 2, pp. 39–41, Feb. 1997.
[5] H. A. Wheeler, "Fundamental limitations of small antennas," *Proc. IRE*, vol. 35, no. 12, pp. 1479–1484, Dec. 1947.
[6] R. C. Hansen, "Fundamental limitations in antennas," *Proc. IEEE*, vol. 69, no. 2, pp. 170–182, Feb. 1981.
[7] S. R. Best, "A discussion on the quality factor of impedance matched electrically small wire antennas," *IEEE Trans. Antennas Propag.*, vol. 53, no. 1, pp. 502–508, Jan. 2005.
[8] J. T. Merenda, "Synthesizer radiating systems and methods," U.S. Patent 5,402,133, Mar. 28, 1995.
[9] J. T. Merenda, "Digital wideband small antenna systems," *IEEE Antennas Propag. Mag.*, vol. 48, no. 5, p. 105, Oct. 2006.
[10] "Max961 single, ultra-high-speed, $+3\,V/+5\,V$, beyond-the-rails comparator (datasheet)," Maxim, Sunnyvale, CA, Tech. Rep., 2007.
[11] C. J. Chu, "Physical limitations of omnidirectional antennas," *J. Appl. Phys.*, vol. 19, pp. 1163–1175, Dec. 1948.
[12] G. W. Streable and L. W. Pearson, "A numerical study on realizable broad-band and equivalent admittances for dipole and loop antennas," *IEEE Trans. Antennas Propag.*, vol. AP-29, no. 5, pp. 707–717, Sep. 1981.
[13] T. G. Tang, Q. M. Tieng, and M. W. Gunn, "Equivalent circuit of a dipole antenna using frequency-independent lumped elements," *IEEE Trans. Antennas Propag.*, vol. 41, no. 1, pp. 100–103, Jan. 1993.
[14] S. A. Schelkunoff and H. T. Friis, *Antennas—Theory and Practice*. New York: Wiley, 1952.
[15] M. Kanda, "Analytical and numerical techniques for analyzing an electrically short dipole with a nonlinear load," *IEEE Trans. Antennas Propag.*, vol. AP-28, no. 1, pp. 71–78, Jan. 1980.
[16] S. B. Wang, A. M. Niknejad, and R. W. Brodersen, "Modeling omnidirectional small antennas for uwb applications," in *IEEE AP-S Int. Symp. Conf. Rec.*, 2004, pp. 1295–1298.

Steven D. Keller (M'01) ▮▮▮▮▮▮ He received the B.S. degree in electrical and computer engineering from Cornell University, Ithaca, NY, in 2004, and the M.S. and Ph.D. degrees in electrical and computer engineering from Duke University, Durham, NC, in 2006 and 2008, respectively.

From 2002 to 2004, he was a Summer Intern with the Air Traffic Control Division, Sensis Corporation, Dewitt, NY. In 2006 and 2007, he was a Summer Intern with the Antennas and RF Technology Branch, Sensors and Electron Devices Directorate, U.S. Army Research Laboratory (ARL), Adelphi, MD. Since 2008, he has been an Electronics Engineer with the ARL, where he conducts research on electronic scanning arrays for SATCOM and radar systems, electrically small and low-profile/conformal antennas, and novel materials for antenna design.

W. Devereux Palmer (S'89–M'91–SM'01) received the Ph.D. degree in electrical engineering from Duke University, Durham, NC, in 1991

He is currently a Program Manager with the U.S. Army Research Office, Research Triangle Park NC, where he is responsible for extramural basic research in computational electromagnetics, antennas, RF circuit integration, and power electronics. From 1991 to 2001, he was a Member of Technical Staff with the MCNC Research and Development Institute. He is currently engaged in antenna research as a member of the Duke University Graduate Faculty and occasionally teaches introductory electromagnetics.

Dr. Palmer is a Registered Professional Engineer in the State of North Carolina. Since 2009, he has been chair of the Eastern NC Section.

William T. Joines (M'61–SM'94–LSM'97–LF'08) was born in Granite Falls, NC. He received the B.S.E.E. degree (with high honors) from North Carolina State University, Raleigh, in 1959, and the M.S. and Ph.D. degrees in electrical engineering from Duke University, Durham, NC, in 1961 and 1964, respectively.

From 1959 to 1966, he was a Member of Technical Staff with Bell Telephone Laboratories, Winston-Salem, NC, where he was engaged in research and development of microwave components and systems for military applications. In 1966, he joined the faculty of Duke University, where he is currently a Professor of electrical and computer engineering. He has authored or coauthored over 100 technical papers on electromagnetic-wave theory and applications. He holds 20 U.S. patents. His research and teaching interests are in the area of electromagnetic-wave interactions with structures and materials, mainly at microwave and optical frequencies.

Dr. Joines was the recipient of the Scientific and Technical Achievement Award presented by the Environmental Protection Agency in 1982, 1985, and 1990.